DOI: 10.1002/ejic.201000661

Reversible, Fine Performance Tuning of an Organometallic Molecular Wire by Addition, Ligand Replacement and Removal of Dicobalt Fragments

Yuya Tanaka,[a] Takashi Koike,[a] and Munetaka Akita*[a]

Keywords: Metal–metal interactions / Mixed-valent compounds / Molecular devices / Molecular wires / Organometallic compounds

Communication between the two iron centres in (dithienylethyne)diyl complex **1** can be finely tuned by reversible addition to, ligand replacement at and removal from the C≡C moiety in **1** of dicobalt fragments $Co_2(CO)_n(PR_3)_{6-n}$. Performance analysis reveals that disparate mechanisms are in operation for the two systems. In the case of the dicobalt adducts, indirect communication via the dicobalt steppingstone can be finely tuned by controlling the electronic structure of the dicobalt unit.

Introduction

Downsizing is one of key issues in modern electronic science and industry, [1] and, as one of effective bottom-up strategies for this issue, molecular electronics has attracted increasing attention. If functions of an electronic circuit can be represented by a combination of molecular components, one would be able to obtain a circuit miniaturized to a minimal level. A number of studies have been conducted toward this goal, and, in organic-based systems, π-conjugated systems play central roles as devices carrying electrons and holes.[2] Furthermore, combination with metal fragments renders the systems more sophisticated, thanks to their unique properties such as redox and magnetic features. Organometallic molecular wires consisting of redox-active metal centres connected by a π-conjugated bridge have been studied extensively; as a result, many excellent molecular wires with strongly interacting metal centres (e.g. polyynediyl complexes) have been developed so far.[3] In addition to the most basic component, that is, wires, fine tuning of the electronic communication between two or more remote redox-active sites is demanded to develop molecular parts such as switches, resistors and diodes.[4] Recently, efficient ON/OFF-type *switches* based on photo-, pH- and ionochromic linkers have been developed by several research groups including our group.[5–7]

Herein we describe reversible, fine tuning of the performance of an acetylene-based diiron molecular wire (Scheme 1). To achieve the desired functions, the molecule should be stable in at least three different states that can be interconverted to each other. We have chosen "coordination" to control the communication between the two metal centres (Scheme 1) and picked up an acetylene-based diiron molecular wire, **1** (Scheme 2), in which (i) the communication may be controlled by addition of dicobalt species to the C≡C moiety and (ii) the effects brought about by the dicobalt fragment can be further finely tuned by introducing appropriate ligands to it. The present study has also revealed that different communication mechanisms operate for **1** and its dicobalt adducts.

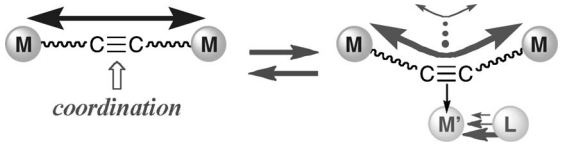

Scheme 1. Reversible, fine tuning of metal–metal interaction.

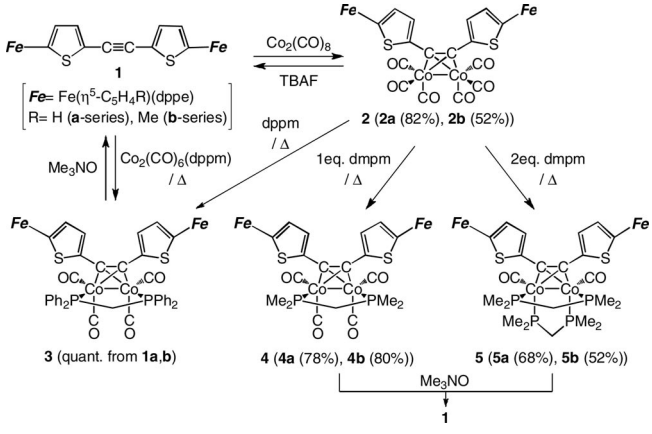

Scheme 2. Synthesis of dicobalt adducts of **1**.

[a] Chemical Resources Laboratory, Tokyo Institute of Technology, R1-27, 4259 Nagatsuta, Midori-ku, Yokohama 226-8503, Japan
Fax: +81-45-924-5230
E-mail: makita@res.titech.ac.jp

Supporting information for this article is available on the WWW under http://dx.doi.org/10.1002/ejic.201000661.

Results and Discussion

A diiron complex with the (dithienylethyne)diyl bridge, [*Fe*–Th–C≡C–Th–*Fe*] (**1**) {*Fe* = Fe(η^5-C_5H_4R)(dppe); R = H (**a**-series), Me (**b**-series); Th = thiophene-2,5-diyl}, was prepared by lithiation of bis(thien-2-yl)ethyne followed by metalation with I-Fe(η^5-C_5H_4R)$(CO)_2$ and photochemical ligand substitution with dppe.[8] (The **b**-series derivatives were prepared in order to avoid the solubility problem.) X-ray crystallographic analysis of **1b** (Figure 1) reveals the coplanar conformation of the two thiophene rings and an Fe···Fe separation of 12.7 Å.[9] Cobalt adducts **2** and **3** were obtained by reaction of **1** with [$Co_2(CO)_8$] and [$Co_2(CO)_6$-(dppm)], respectively, in thf at room temperature.[10] Ligand replacement of **2** with bidentate phosphanes [$R'_2PCH_2PR'_2$: R′ = Ph(dppm), Me(dmpm)] gave the mono- (**3**, **4**) and disubstituted (**5**) products. All complexes show single sets of NMR spectroscopic signals for the η^5-C_5H_4R (^{1}H) and dppe ligands (^{31}P) at room temperature, indicating symmetrical structures for **1**–**5** and the occurrence of fluxional behaviour of the ligands attached to the Co centres in **3**–**5**.

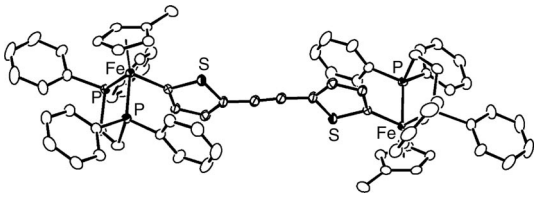

Figure 1. An ORTEP view of **1b** drawn with thermal ellipsoids at the 30% probability level. Hydrogen atoms are omitted for clarity.

Electron densities at the Fe and Co centres are estimated by CV and IR spectroscopic measurements. Two Fe-centred redox waves appear in the range –1200 to –400 mV (Table 1).[11] Attachment of the $Co_2(CO)_6$ fragment to **1a** causes slight anodic shifts of $E_{1/2}^{Fe1}$ and $E_{1/2}^{Fe2}$ (the first and second redox potential for the iron centres, respectively), whereas ligand replacement of the resultant adduct **2a** by the electron-donating diphosphane ligands causes significant cathodic shifts of $E_{1/2}^{Fe1}$ and $E_{1/2}^{Fe2}$ (increasing order of the electron densities at the Fe centres: **2a** < **3a** < **4a** < **5a**) in accord with the increasing order of the electron densities at the dicobalt centres estimated on the basis of the shifts of the CO vibrations to lower energies [ν_{CO} (KBr): 2067, 2033, 2001 (**2a**), 2009, 1984, 1957 (**3a**), 2001, 1972, 1945 (**4a**), 1898 (**5a**) cm^{-1}] as well as the cathodic shifts of the Co-centred redox processes ($E_{1/2}^{Co}$).

Communication performance of the obtained complexes is evaluated on the basis of IVCT bands (MMCT appearing in the near IR region) of *1e-oxidized monocationic species*.[12] In particular, the V_{ab} coupling value, which is derived from the spectral parameters of the IVCT bands, represents the extent of electronic interaction between the two redox-active metal centres.[12c] A high-performance organometallic molecular wire shows a large V_{ab} value associated with an intense, sharp IVCT band (with a large ε_{max} and a small $\nu_{1/2}^{exp}$).[12a] Prior to the determination of the V_{ab} value, it is essential to classify the compound into one of three classes (Robin–Day Classes I–III), because different equations are applied to obtain the V_{ab} value (see footnotes [c,d] of Table 1); two V_{ab} values for Class II and III compounds are shown in Table 1.[13] For the Robin–Day classification, solvent dependency and half-height width of the IVCT band are critical factors.[12c] For a high-performance Class III compound, (1) the absorption maximum (ν_{max}) of the IVCT band is little affected by the solvent polarity, and (2) the half-height width thereof ($\nu_{1/2}^{exp}$) is narrower than the value predicted on the basis of the Hush theory ($\nu_{1/2}^{calc}$). Comparison of the performances of compounds belonging to different classes should be made with care by taking into account the above-mentioned factors. Monocationic complexes **1a**$^+$, **3a**$^+$, **4a**$^+$ and **5a**$^+$ were obtained by chemical 1e-oxidation of the corresponding neutral complexes with 1 equiv. of [$FeCp_2$][PF_6], whereas the thermodynamically less stable **2a**$^+$ was generated in situ by comproportionation of the isolable neutral (**2a**) and dicationic species (**2a**$^{2+}$).[8]

Complex **1a**$^+$ shows intense NIR bands in the region 3000–8000 cm^{-1} (Figure 2a), which are attributed to the Fe-to-Fe IVCT bands, as noted for the related Fe(η^5-C_5R_5)(dppe) complexes.[3a,14] These NIR bands have been successfully deconvoluted into three Gaussian curves, of which the most intense, lowest energy band (band I; ν_{max} = 4240 cm^{-1}) is used for the determination of V_{ab}.[3a,14] Because (1) ν_{max} of this IVCT band is little affected by the solvent polarity (less than 100 cm^{-1})[8,12c,15] and (2) the half-height width of this band ($\nu_{1/2}^{exp}$ = 1220 cm^{-1}) is signifi-

Table 1. Electrochemical and NIR data for complexes **1a**–**5a**.[a]

Complex	$E_{1/2}^{Fe1}$ /mV	$E_{1/2}^{Fe2}$ /mV	$E_{1/2}^{Co}$ /mV	$\Delta E^{Co/Fe2}$ /mV	ν_{max} /cm^{-1}	ε_{max} /M^{-1} cm^{-1}	$\nu_{1/2}^{exp}$ /cm^{-1}	$\nu_{1/2}^{calcd.[b]}$ /cm^{-1}	$V_{ab}^{II\ [c]}$ /cm^{-1}	$V_{ab}^{III[d]}$ /cm^{-1}
1a	–620	–432	–	–	4240	22320	1220	3130	551	2120
2a	–595	–483	>400 [e]	>883	7650	1900	2646	4204	550	3825
3a	–736	–571	21	592	8295	5120	3562	4377	1091	4148
4a	–755	–567	–112	455	7660	5380	3086	4206	1000	3830
5a	–1039	–681	–312	369	6060	10660	2550	3741	1138	3030

[a] The CV data are for the neutral species, and the NIR spectroscopic data are for the corresponding monocationic species. Conditions for electrochemical measurements: [complex] = ≈ 1.0×10^{-3} M, [NBu_4·PF_6] = 0.1 M at 293 K, scan rate = 100 mV/sec. $E_{1/2}$ values are referenced against the $FeCp_2$/[$FeCp_2$]$^+$ couple. $E_{1/2}^{Fe1}$, $E_{1/2}^{Fe2}$ and $E_{1/2}^{Co}$ are the first and second redox potentials for the iron centres and the redox potential for the dicobalt centre, respectively. $\Delta E^{Co/Fe2}$ is the difference between $E_{1/2}^{Co}$ and $E_{1/2}^{Fe2}$. [b] $\nu_{1/2}^{calcd.}$ (in cm^{-1}) = $(2310 \cdot \nu_{max})^{1/2}$. [c] V_{ab}^{II} (estimated as a Class II compound) = 2.06×10^{-2} (ν_{max} =·ε_{max}·$\nu_{1/2}^{exp})^{1/2}$·r^{-1} (r: M···M distance).[9] [d] V_{ab}^{III} (estimated as a Class III compound) = (1/2)·ν_{max} =. [e] The $E_{1/2}^{Co}$ process overlaps with the Fe^{III}–Fe^{III}/Fe^{III}–Fe^{IV} process.

cantly narrower than the predicted value ($\nu_{1/2}^{calc}$ = 3130 cm^{-1}),[13] it is concluded that complex **1a**$^+$ falls in the Robin–Day Class III (fully delocalized system) with an V_{ab} value of 2120 cm^{-1}, and thus the two metal centres therein strongly interact with each other.

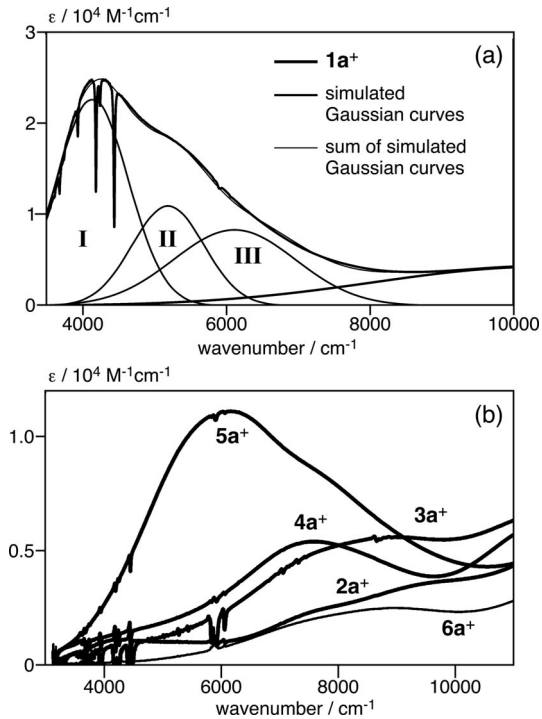

Figure 2. (a) NIR spectrum for **1a**$^+$ and its deconvoluted Gaussian curves and (b) NIR spectra for **2a**$^+$–**6a**$^+$ (observed in CH_2Cl_2).

Cobalt adducts **2a**$^+$–**5a**$^+$ exhibit IVCT bands that are remarkably different from those of **1a**$^+$ (Figure 2b; the absorptions at greater than 10000 cm^{-1} are LMCT bands), because of the different IVCT mechanisms (see below). For example, the IVCT bands for **2a**$^+$–**5a**$^+$ are considerably weaker than those of **1a**$^+$, and the absorption maxima (ν_{max}) are shifted to higher energies. The order of the solvent dependency is determined to be as follows: **3a**$^+$ > **4a**$^+$ > **5a**$^+$[8] (**2a**$^+$ can not be examined because of its low stability).

Compound **5a**$^+$ has been assigned to Class IIB, although the little solvent dependency and the half-height width ($\nu_{1/2}^{exp}$) of the IVCT band narrower than $\nu_{1/2}^{calc}$ suggest its assignment to Class III. One debatable point is the considerably large $\nu_{1/2}^{exp}$ value (2550 cm^{-1}) compared to those of typical Class III compounds (e.g. **1a**$^+$: 1220 cm^{-1}). Recently, this type of compounds has been categorized into the subclass "Class IIB", as discussed by Brunschwig et al.,[12b] that is, the electronic coupling is underestimated by the Hush treatment (V_{ab}^{II}) and overestimated by the Class III treatment (V_{ab}^{III}).[14a]

The solvent-dependent species **2a**$^+$–**4a**$^+$ belong to Class II (Table 1). Complex **2a**$^+$ shows the smallest V_{ab}^{II} value (550 cm^{-1}). Although the V_{ab}^{II} values for **3a**$^+$ (1091 cm^{-1}) **4a**$^+$ (1000 cm^{-1}) and **5a**$^+$ (1138 cm^{-1}) are comparable, a monotonous increase of ε_{max} and a monotonous decrease of $\nu_{1/2}^{exp}$ are noted for the series **2a**$^+$–**5a**$^+$ with the only exception of $\nu_{1/2}^{exp}$ of **2a**$^+$. Because high performance is associated with an intense, sharp IVCT band (with a large ε_{max} and a small $\nu_{1/2}^{exp}$) leading to a large V_{ab} value, the two factors (ε_{max} and $\nu_{1/2}^{exp}$) are also considered to be criteria for the classification. The monotonous changes of ε_{max} and $\nu_{1/2}^{exp}$ and the Class III performance of **1a**$^+$ discussed above (with by far the largest ε_{max} and smallest $\nu_{1/2}^{exp}$ values) reveal the order of the wire-like performance as follows: **1a**$^+$ (Class III) >> **5a**$^+$ (Class IIB) > **4a**$^+$ > **3a**$^+$ > **2a**$^+$ (Class IIA). This order turns out to be consistent with that estimated on the basis of the ESR parameters for **1a**$^+$–**5a**$^+$,[16,17] and can furthermore be correlated to the increasing order of the electron densities at the Co centres discussed above.

Thus, the communication between the two iron centres can be controlled by coordination of the dicobalt species to the C≡C moiety in **1** and can be further tuned by introduction of a phosphane ligand with the appropriate electron-donating ability.

The attached dicobalt fragments in **2**–**5** can be removed upon treatment with NBu_4F or O←NMe_3 (Scheme 2).[20] Thus, the dicobalt fragment can be attached to and removed from **1** in a reversible manner. In other words, the wire-like performance of the organometallic molecular wire **1** can be controlled by addition, ligand substitution and removal of the dicobalt unit.

The significantly different features of the IVCT bands observed for **1a**$^+$ and **2a**$^+$–**5a**$^+$ suggest disparate mechanisms operating for the two systems. The IVCT band for **1a**$^+$ arises from the Fe-to-Fe MMCT, because **1a**$^+$ contains the two iron centres as the unique redox-active sites. On the other hand, two pathways are feasible for the dicobalt adducts **2a**$^+$–**5a**$^+$, that is, the direct Fe–Fe MMCT as observed for **1a**$^+$ and the indirect Fe–Co–Fe MMCT, where the dicobalt unit works like a steppingstone. Of the two mechanisms, it turns out that the latter process is at work for **2a**$^+$–**5a**$^+$, because monocationic species [(μ-η^2:η^2-*Fe*–Th–C≡C–Th–H)$Co_2(CO)_4$(dppm)] (**6a**), a monoiron derivative of **3a**, for which *direct Fe–Fe transition is not feasible but Fe–Co transition is feasible*, has a NIR absorption band that is close in shape to that of **3a**$^+$ (Figure 2b). It should be also noted that (1) ε_{max} of the monoiron species **6a**$^+$ is about half of that of the diiron species **3a**$^+$ (Figure 2b) and (2) the transition is characterized as an IVCT band as revealed by the linear relationship between ν_{max} and ($1/n^2 - 1/D_s^2$) observed in solvents with different polarities (n and D_s are denoted by the optical and statistical dielectric constants of the solvent).[8,21]

Electron transfer process of dinuclear species has been interpreted in terms of the diagram involving two overlapping potential energy curves.[22] A simplified diagram for a Class II dinuclear species is shown in Scheme 3a. Photochemical excitation of the ground state A by absorption of the IVCT transition energy (ν_{IVCT}) and subsequent thermal relaxation following the potential curve finally lead to B to accomplish the electron transfer between the two iron centres. For the three-component dicobalt adducts **2**–**5**,

electron transfer can be explained by the potential energy curve diagrams shown in Scheme 3b.[23] The IVCT transition from the ground state C followed by thermal relaxation in a manner similar to the dinuclear system leads to the intermediary state D. Subsequent thermally induced electronic transition from the other iron centre to the dicobalt unit leads to the other ground state E to accomplish the electron transfer between the two iron centres via the dicobalt unit. In this context, the energy gap (ΔE) is a key factor for the determination of V_{ab}, because a diminution of ΔE brings about an increase in the electronic coupling V_{ab}. ΔE can be experimentally estimated by the CV data, that is, ΔE is equivalent to the difference of the redox potentials for the iron and cobalt centres ($\Delta E^{Co/Fe2}$).[24] As summarized in Table 1, the order of the $\Delta E^{Co/Fe2}$ values are **2a** > **3a** > **4a** > **5a**. Thus a compound with a small $\Delta E^{Co/Fe2}$ value gives a large V_{ab} value (**5a** > **4a** > **3a** > **2a**), in accord with the experimental results described above. As a result of these electronic effects, the communication performance (V_{ab}) of the dicobalt adducts can be finely tuned by choosing a ligand with appropriate electron-donating ability. ΔE can be correlated to the densities at the dicobalt unit, which can be estimated by $E_{1/2}^{Co}$ and ν_{CO} as discussed above; in other words, an electron-donating ligand induces better communication between the two metal centres.

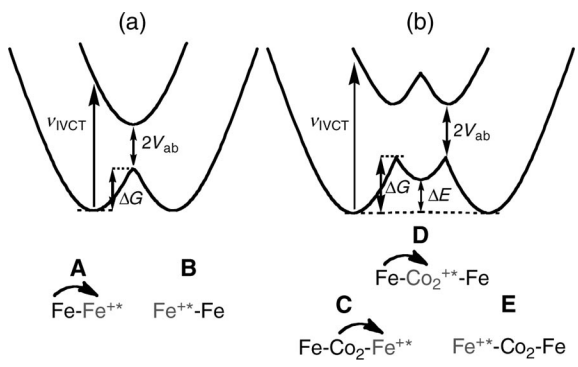

Scheme 3. Energy diagrams for (a) di- and (b) tricomponent systems of Class II. V_{ab}: electronic coupling; ν_{IVCT}: IVCT transition energy; ΔE: energy gap between the Fe and Co centres; ΔG: thermal electron-transfer barrier.

Conclusions

We have succeeded in fine tuning the communication between the two metal centres in the organometallic molecular wire **1** by attachment and removal of an appropriate dicobalt fragment (Scheme 1). It is notable that: (1) the wire-like performance of the derivatives varies in the range from Robin–Day Class IIA (**2**) to Class III (**1**); and (2) **1** and the cobalt adducts **2**–**5** can be interconverted in a reversible and facile manner. In the case of the dicobalt adducts, the indirect communication via the dicobalt steppingstone can be finely tuned by controlling the electronic structure of the dicobalt unit.

CCDC-775289 (**1b**) contains the supplementary crystallographic data for this paper. These data can be obtained free of charge from The Cambridge Crystallographic Data Centre via www.ccdc.cam.ac.uk/data_request/cif.

Supporting Information (see footnote on the first page of this article): Full synthetic and spectroscopic details of **1**–**5**.

Acknowledgments

The financial support from the Japanese government (Grants-in-Aid for Scientific Research: Nos. 18065009, 20044007 and 50167839; M. A.) and the Japan Society for the Promotion of Science (Y. T.) are gratefully acknowledged. We are also grateful to Dr. F. Paul (University of Rennes 1) for the helpful discussion on the ESR analysis.

[1] J. Jortner, M. A. Ratner, *Molecular Electronics*, Blackwell Science, Oxford, **1997**; A. Aviram, M. Ratner, *Ann. NY Acad. Sci.* **1998**, 852; M. Ratner, *Nature* **2000**, *404*, 137; B. L. Feringa (Ed.), *Molecular Switches*, Wiley-VCH, Weinheim, **2001**; J. M. Tour, *Acc. Chem. Res.* **2000**, *33*, 791; N. Robertson, G. A. Mc Gowan, *Chem. Soc. Rev.* **2003**, *32*, 96; M. A. Reed, T. Lee (Eds.), *Molecular Nanoelectronics*, American Scientific Publishers, Stevenson Ranch, CA, **2003**; M. C. Petty, *Molecular Electronics: From Principles to Practice*, Wiley, New York, **2008**; K. Szacilowski, *Chem. Rev.* **2008**, *108*, 3481.

[2] V. Coropceanu, J. Cornil, D. A. S. Filho, Y. Olivier, R. Silbey, J.-L. Brédas, *Chem. Rev.* **2007**, *107*, 926.

[3] a) F. Paul, C. Lapinte, *Coord. Chem. Rev.* **1998**, 178–180; F. Paul, C. Lapinte, *Coord. Chem. Rev.* **1998**, 427; b) M. I. Bruce, P. J. Low, *Adv. Organomet. Chem.* **2004**, *50*, 231; c) S. Szafert, J. A. Gladysz, *Chem. Rev.* **2006**, *106*, PR1; d) T. Ren, *Chem. Rev.* **2008**, *108*, 4185–4207; e) M. Akita, T. Koike, *Dalton Trans.* **2008**, 3523; f) P. F. H. Schwab, M. D. Levin, J. Michl, *Chem. Rev.* **1999**, *99*, 1863; g) P. F. H. Schwab, J. R. Smith, J. Michl, *Chem. Rev.* **2005**, *105*, 1197.

[4] C. Joachim, J. K. Gimzewski, A. Aviram, *Nature* **2000**, *408*, 541; M. Irie, *Chem. Rev.* **2000**, *100*, 1685.

[5] S. Fraysee, C. Coudret, J.-P. Launay, *Eur. J. Inorg. Chem.* **2000**, 1581; G. Guirado, C. Christophe, J.-P. Launay, *J. Phys. Chem. C* **2007**, *111*, 2770; Y. Tanaka, T. Koike, M. Akita, *Chem. Commun.* **2007**, 1169; K. Motoyama, T. Koike, M. Akita, *Chem. Commun.* **2008**, 5812; Y. Liu, C. Lagrost, K. Costuas, N. Touchar, H. Le Bozec, S. Rigaut, *Chem. Commun.* **2008**, 6117; Y. Lin, J. Yuan, M. Hu, J. Cheng, J. Yin, S. Jin, S. H. Liu, *Organometallics* **2009**, *28*, 6402.

[6] H. Tannai, K. Tsuge, Y. Sasaki, *Inorg. Chem.* **2005**, *44*, 5206; C. D. Pietro, S. Campagna, M. T. Gandolfi, R. Ballardini, S. Fnni, W. R. Browne, J. G. Vos, *Inorg. Chem.* **2002**, *41*, 2871; M. Haga, M. M. Ali, S. Koseki, K. Fujimoto, A. Yoshimura, K. Nozaki, T. Ohno, K. Nakajima, D. J. Stufkens, *Inorg. Chem.* **1996**, *35*, 3335.

[7] Y. Ie, T. Kawabata, T. Kaneda, Y. Aso, *Chem. Lett.* **2006**, *35*, 1366.

[8] See Supporting Information.

[9] Crystallographic data for **1b**: $C_{78}H_{74}Cl_8Fe_2P_4S_2$ (**1b**·$4CH_2Cl_2$), M_r = 1594.67; triclinic space group $P\bar{1}$; a = 9.3537(13) Å, b = 12.1333(15) Å, c = 17.988(2) Å; α = 81.632(6)°; β = 84.916(6)°; γ = 67.604(5)°; V = 1866.1(4) Å^3; Z = 1; $\rho_{calcd.}$ = 1.419 g cm^{-3}; μ = 0.860 mm^{-1}; λ = 0.71073 Å; T = –60 °C; total data collected = 15426; $R1$ = 0.0538 [5126 observed reflections with $F_o^2 > 2\sigma(F_o^2)$]; $wR2$ = 0.1520 for 424 variables and all 7796 unique reflections.

[10] Preliminary X-ray crystallographic structure analysis of **3b** revealed the equatorial coordination of the dppm ligand as well as the value of 7.34 Å (r for the dicobalt adducts; Table 1) for the average Fe···Co separation.

[11] K_C (comproportionation constant) values are as follows: ΔE (in mV)/K_C = 188/1.5 × 10^3 (**1a**), 112/79 (**2a**), 165/6.1 × 10^2 (**3a**), 189/1.5 × 10^3 (**4a**), and 358/1.1 × 10^6 (**5a**).

[12] a) N. S. Hush, *Prog. Inorg. Chem.* **1967**, *8*, 391; b) B. S. Brunschwig, C. Creutz, N. Sutin, *Chem. Soc. Rev.* **2002**, *31*, 168; c) K. D. Demadis, C. M. Hartshorn, T. J. Meyer, *Chem. Rev.* **2001**, *101*, 2655.
[13] C. Creutz, H. Taube, *J. Am. Chem. Soc.* **1969**, *91*, 3988.
[14] a) S. I. Ghazala, F. Paul, L. Toupet, T. Roisnel, P. Hapiot, C. Lapinte, *J. Am. Chem. Soc.* **2006**, *128*, 2463; b) F. de Montigny, G. Argouarch, K. Costuas, J.-F. Halet, T. Roisnel, L. Toupet, C. Lapinte, *Organometallics* **2005**, *24*, 4558; c) Y. Tanaka, J. A. Shaw-Taberlet, F. Justaud, O. Cador, T. Roisnel, M. Akita, J.-R. Hamon, C. Lapinte, *Organometallics* **2009**, *28*, 4656.
[15] S. Stang, F. Paul, C. Lapinte, *Organometallics* **2000**, *19*, 1035.
[16] P. Hamon, F. Justaud, O. Cador, P. Hapiot, S. Rigaut, L. Toupet, L. Ouahab, H. Stueger, J.-R. Hamon, C. Lapinte, *J. Am. Chem. Soc.* **2008**, *130*, 17372; T.-Y. Dong, D. N. Hendrickson, C. G. Pierpont, M. F. Moore, *J. Am. Chem. Soc.* **1986**, *108*, 963.
[17] The extent of delocalization of the radical centre over the metal-π-conjugated system can also be estimated on the basis of ESR parameters. Complex **1** displays three components of *g* tensors expected for pseudo-octahedral d^5 low spin Fe^{III} complexes, indicating that the radical cation is mainly localized on the iron centre on the ESR measurement time scale (ca. 10^{-9} s). The cobalt adducts show a couple of slightly broad *g* tensors, which also arise from Fe^{III}. The isotropic *g* value (g_{iso}) and the anisotropy tensor (Δg) are measures for the delocalization. The g_{iso} value is an indicator of the metal character of the SOMO,[18] and Δg decreases as the rate of the intramolecular electron transfer increases in a homologous series of mixed-valence compounds.[19,3a] The tendencies of the two parameters (**1a**$^+$ < **5a**$^+$ < **4a**$^+$ < **3a**$^+$ < **2a**$^+$) are in accord with the result obtained from the NIR spectroscopic data. Δg = 0.213 (**2a**$^+$) > 0.130 (**3a**$^+$) > 0.113 (**4a**$^+$) > 0.091 (**5a**$^+$) > 0.084 (**1a**$^+$); g_{iso} = 2.092 (**2a**$^+$) > 2.068 (**3a**$^+$) > 2.057 (**4a**$^+$) > 2.052 (**5a**$^+$) > 2.042 (**1a**$^+$).
[18] F. D. Montigny, G. Argouarch, K. Costuas, J.-F. Halet, T. Roisnel, L. Toupet, C. Lapinte, *Organometallics* **2005**, *24*, 4558.
[19] T.-Y. Dong, D. N. Hendrickson, C. G. Pierpont, M. F. Moore, *J. Am. Chem. Soc.* **1986**, *108*, 963.
[20] a) D. S. Davis, S. C. Shadinger, *Tetrahedron Lett.* **1999**, *40*, 7749; b) G. B. Jones, J. M. Wright, T. M. Rush, G. W. Plourde II, T. F. Kelton, J. E. Mathews, R. S. Huber, J. P. Davidson, *J. Org. Chem.* **1997**, *62*, 9379.
[21] M. J. Powers, T. J. Meyer, *J. Am. Chem. Soc.* **1978**, *100*, 4393.
[22] R. A. Marcus, N. Sutin, *Biochim. Biophys. Acta* **1985**, *811*, 265.
[23] D. M. D'Alessandro, F. R. Keene, *Chem. Rev.* **2006**, *106*, 2270; Y. Zhu, O. Clot, M. O. Wolf, G. P. A. Yap, *J. Am. Chem. Soc.* **1998**, *120*, 1812; B. W. Pfennig, A. B. Bocarsly, *J. Phys. Chem.* **1992**, *96*, 226.
[24] Because, in general, $E_{1/2}^{Fe1}$ is significantly influenced by the wire-like performance, $E_{1/2}^{Fe2}$, which is hardly affected by the wire-like performance, is used instead.

Received: June 16, 2010
Published Online: July 16, 2010

